OPEN ACCESS

Global Journal of Research in Agriculture & Life Sciences
ISSN: 2583-4576 (Online)
Volume 05 | Issue 05 | Sept.-Oct. | 2025
Journal homepage: https://gjrpublication.com/gjrals/

Research Article

Performance Comparison of Solar Water Heaters with Zigzag and Spiral Tube Configurations Using ANSYS FLUENT

*Zayyanu Hussaini[1] Muktar Muhammad[1], David Daniel[1], Asabe Ibrahim Audu[1] and Rufai Usman Fakai[2]

[1]Department of Physics, Federal University of Agriculture, Zuru (FUAZ).
[2]School of Science, Adamu Augie College of Education, Argungu, Kebbi State, Nigeria.

DOI: 10.5281/zenodo.17119079 **Submission Date:** 02 Aug. 2025 | **Published Date:** 15 Sept. 2025

***Corresponding author:** Zayyanu Hussaini*
Department of Physics, Federal University of Agriculture, Zuru (FUAZ).
https://orcid.org/0009-0005-2955-5899

Abstract

Energy demand is experiencing a significant increase due to the rise in the standard of living and industrial growth in numerous countries. This has led to the emergence of a substantial gap between energy supply and demand. In this work, an attempt has been made to design and evaluate the performance analysis of a solar water heater with different tube arrangements using ANSYS FLUENT. The meteorological data for Sokoto (13° 03' 45.68N, 5° 14' 35.59E) were analyzed to determine the average solar radiation for each month. A numerical study of solar water heaters with various tube configurations has been conducted. The laminar turbulence model is used for flow simulation, whereas the radiation model solver is used to incorporate the radiative element in the energy equation. Based on the findings, it is clear that the solar water heater with the Zigzag tube configuration recorded the highest outlet temperature of 72 °C, a temperature difference of 38 °C, and 60.56% efficiency at approximately 12:00 hours, compared to the solar water heater with a spiral tube layout reached 68 °C and an efficiency of 54.19% at 12:00 hours. Based on these results, it can be assumed that a solar water heater with a Zigzag tube design has the highest performance efficiency compared to a spiral tube design. It may be determined that the tube configuration is very crucial to the operation of a solar water heater. According to the data, at its peak hours, the solar water heater with a spiral tube configuration had the lowest efficiency. The findings above clearly demonstrate that the tube configuration has a significant impact on the performance of solar water heaters. However, it was discovered that solar radiation, the source of thermal energy in the solar collector, was the primary climatic factor affecting the variation in water temperature. The temperature and wind speed of the outside air might affect a collector's thermal losses.

Keywords: *Solar Water heater, ANSYS FLUENT, Spiral, Conventional, CFD.*

Introduction

The world relies heavily on fossil fuels to meet most of its energy demands, and this has caused significant harm to the Earth. The increase in greenhouse gas levels in the atmosphere is primarily attributed to the combustion of fossil fuels as a primary source of energy. This has contributed to global warming, which has led to climate change, increased flooding, forest fires, rising sea levels, and the melting of glaciers. These are just some of the consequences of our over-reliance on fossil fuels for our energy demands. Solar energy provides an alternative and environmentally friendly energy source to the fossil fuels used for our energy needs. Over the last few decades, solar energy systems have gained more recognition because they can provide energy at a low long-term cost and minimal environmental damage. Researchers have developed several techniques for harnessing solar energy; these techniques include applications for space heating, water heating, electricity generation, and many others.

The majority of people living in rural areas encounter frequent power outages due to their remote location from the regular power system, inadequate power outages, and poor power quality. Many people became interested in using fossil fuel generators for alternative purposes as a result of this. Fossil fuel burning is inefficient and may be a factor in climate change. Many countries are interested in renewable energy technology because of the harm that fossil fuels cause to the environment and how they contribute to climate change and global warming. (Kangiwa *et al*, 2023)

Solar energy is generated by the fusion reaction of hydrogen atoms in the sun. This fusion reaction results in the release of high-energy particles called gamma rays. Gamma rays are transmitted as electromagnetic radiation to the Earth, which is about 150 million kilometers from the sun. Electromagnetic radiation comes in three forms: infrared rays, visible light, and ultraviolet rays. Solar energy reaching the Earth's surface can be harnessed directly by using photovoltaics (solar cells) and solar concentrators. Photovoltaics are used for electricity generation, while solar concentrators are used as a source of thermal energy. The utilization of solar energy collectors (concentrators) to transform radiation into heat energy is the basis of solar water heating technology. A simple solar water heater consists of a collector, a tank, and the flow channel through which the working fluid is transported.

Solar water heaters, also known as solar domestic hot water systems, offer a cost-effective solution to create hot water for residential use. They can be utilised in any environment, and their fuel, sunlight, is free. (Gulland, 2012)

Numerous experts have conducted extensive research, both experimental and numerical, to evaluate the performance of solar water heaters. Computational Fluid Dynamics (CFD) can significantly increase heat transfer device performance. Marroquín *et al*. Utilised the AN-SYS simulation program, notably the fluid dynamics (CFD) library. The CFX-Mesh is used for meshing, with elements ranging from 0.004 to 0.08 m and a resolution angle of 30°. The simulation uses the k-epsilon energy model to account for turbulent flow, yielding a 5% variation from the experiment.

Islam *et al*. (2019) analysed a solar water heater using water glycerin and discovered that it had the highest efficiency and outlet temperature.

Michaelides used CFD simulations to compare SWH and solar space heating systems. This helped discover and optimise the best system design for Cyprus.

In their study, Eswaran *et al*. (2014) numerically analysed and carried out a reengineered Ado-Ekide solar water heater using CFD and an experimental study, and the results showed that the CFD result achieved maximum mass flow rate compared to the experimental result. The findings demonstrated that these systems can achieve a maximum mass flow rate of 0.6 kg/s. (Belkassmi *et al*. 2021) Numerically investigated how the employment of copper/water, copper oxide/water, and alumina/water nanofluids affected the functioning of an FPC. The average increases in thermal efficiency with copper/water, copper oxide/water, and alumina/water, respectively, were reported by the authors to be 4.44%, 4.27%, and 4.21%.

Methodology

This part encompasses the research design employed in the study, the geographical location where the study took place, the materials utilized, the methodologies employed for data collection, and the methods utilized to evaluate the performance of the solar water heaters.

Methods

This part starts with designing geometries using MODELAR in ANSYS. The geometry for all three systems was designed and meshed using ANSYS software. To start a new project in ANSYS Workbench, navigate to the "File" menu and select "New Project." In the Design Modeler, fluid flow was chosen as the analysis type, utilizing the ANSYS Workbench geometry modeling environment. The dimensions and specifications are listed in Table 1. This step specifies and assigns geometric parameters, including lengths, angles, and distances, to fully specify the models. The geometry quality was verified for faults and inconsistencies. Model finite element analysis was performed using ANSYS Workbench V2021 R2 structural analysis software. We employ transient state thermal analysis and make small changes to the collector model, using aluminium alloy and copper as materials.

ANSYS FLUENT software was used to numerically examine the performance of the solar water heater under identical meteorological conditions. An overarching algorithm exists for all fluid flow issues in ANSYS FLUENT. This algorithm provides an overview of the procedures needed to conduct our numerical simulations of real-world flow problems. Nonetheless, the particulars of the flow problem under simulation affect the choices taken at different times in the simulation.

Table1. Geometrical and Operating Parameters

Dimensions of Tubes	Dimension of shell body (mm)	Length/Quantity (mm)	Material
Storage tank	30	1000	
Pipe	60	2000	Copper
Inlet and outlet diameter	80	30	
Receiver plate	2000x2000	10 thickness	
Evacuated tube	Outer 80 Inner 60	1800	Glass
Fluid domain			Water
Plate			Steel
Mesh		871702	Tetrahedral
Nodes		191418	
Elements		871702	
Iterations		600	

Simulation Setup

The numerical solutions of the governing equations are found using ANSYS. The solar water heater geometry is represented in the design modular; discretization of the computational domain is also done in the ANSYS meshing package, and the solutions are derived in the ANSYS Fluent. The solution is retrieved from the resulting bundle of ANSYS. The governing equations and boundary conditions are solved using the finite volume method, which is implemented in the ANSYS Fluent code. A pressure-based solver is used in this work. As part of the ANSYS Fluent Code's solution approach, the second-order upwind scheme is employed to integrate the governing equations with boundary conditions on the computer platform. The pressure-velocity coupling is employed for the SIMPLE algorithm. The discrete ordinate model is used to simulate radiation heat transfer within the receiver tube‘s annulus space, taking air as a non-participating medium; consequently, it is surface-to-surface radiation heat transfer. It is therefore assumed that air does not absorb, emit, or disperse radiation in the evacuated tube. The realizable k.-e is more advanced than the ordinary realizable k.-e model; it also delivers more accurate forecasts than the Reynolds stress model. The realizable k.-e is more sophisticated than the ordinary realizable k.-e model; it also delivers more accurate forecasts than the Reynolds stress model. It is consequently selected for turbulence modelling. The strengthened wall is specifically intended for the near-wall region. The convergence is monitored by setting the sealed residuals to less than 10^{-4} for continuity, while for momentum, turbulent kinetic energy (k) and turbulence dissipation rate (e) are less than 10^{-5}, and energy residuals are set to be less than 10^{-7}. The solution is executed more than 150 successive iterations until the scaled residual has ceased to change. At this point, the solution converged. Crafting and analysing a solar water heater in ANSYS Fluent involve numerous steps, such as constructing the geometry, arranging the simulation, outlining the boundary conditions, and dissecting the outcomes. General set-up and transient were picked, and the pressure-based absolute velocity formulation was also selected. The energy equation was engaged, and the flow was selected as laminar. For pressure, momentum, and energy, a second-order upwind equation was also used.

The Pre-processing Stage

This is the initial stage of the ANSYS FLUENT simulation process, which aids in providing the most accurate geometry description.

Solver

As a steady state conjugate heat transfer problem, the computational domain has been addressed, and the process of solution is carried out until convergence and an accurate mass and energy balance are attained. The iterative approach involves solving each problem repeatedly for a predetermined amount of time until the convergence requirements are satisfied. The heat balance equation (Energy-on) is used to calculate the heat transfer between the light-absorbing surface and the air. To increase the quality of boundary-layer computation, the Navier-Stokes equation is closed by the usual k-k-model with better wall functions. The Solar Calculator in ANSYS is used to compute the quantity of solar radiation, which allows the intensity of solar radiation to be determined. A second-order upwind approach is used to solve the system of differential equations representing heat and mass transport processes. A convergence criterion of 10^{-6} was set based on concerns of minimising computing calculations. There have been 600 iterations, as stated in Table 1. The convergence of the solution under varied situations occurs between 350 and 500 iterations. However, after the physics problem has been recognised, the following procedures are used to address it using a computer: fluid material attributes, flow physics model, and boundary conditions.

Post processing

After receiving the results, the next step is to analyse them using various techniques, such as contour plots, streamlines, vector plots, etc.

Boundary Conditions Setup

The working fluid is water, and the wall material is copper. A steady-state analysis is performed. The outside temperature and pressure are 300K. The following boundary conditions apply to both absorber tubes. The water's inlet temperature is 300 K. The velocity of the water flowing within the absorber tube is varied from 0.1 to 2.0m/s. At each point, the water's outlet temperature is almost equal to the inlet temperature. The water is given inlet boundary conditions (Temperature and Velocity). Discrete ordinates were enabled in the radiation panel, and the coordinate for Sokoto was set. It was determined that the inlet's mass flow rate was 0.033 kg/s. The working conditions are given in Table 1.

Initialization

Two different kinds of initialisation methods exist. Standard initialisation and hybrid initialisation. In this research, the standard initialisation is employed. The fluid (water) is employed as a reference frame, and the values are computed from the inlet temperature.

Geometry

Geometry is a very important parameter in designing a model in ANSYS software. The solar water heater system was created as shown in Figures 2, 3, and 4, including the solar collector, pipes, and storage tank. The Figures show unstructured meshes in the ANSYS Fluent workbench.

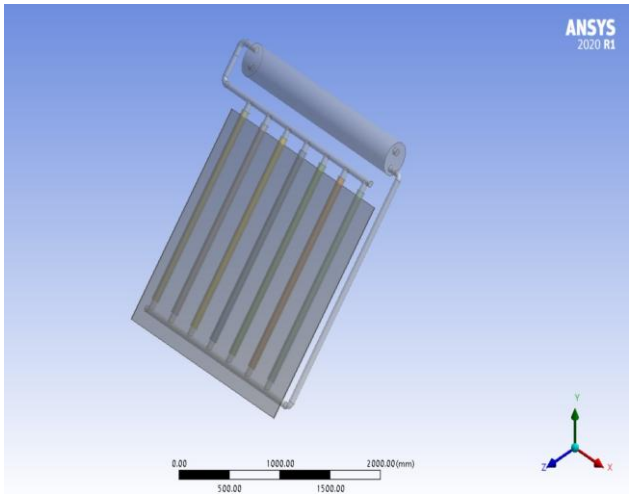

Figure 2: Geometry part of the conventional solar water heater

Meshing Generation

Meshing with high smoothing is done. The technique of splitting the geometric shape into a number of elements and nodes is known as meshing. As a result, when a load is applied to a geometric shape, the load can be distributed uniformly to the geometric shape. The more elements and nodes suggested, the smaller the elements, and therefore the more accurate the findings, but the longer it takes. In contrast, having too few components will result in inaccurate findings. By using size methods that enable more node points near the wall, the usage of structured mesh elements at the wall provides for high resolution of the boundary layer and temperature field gradients. This is especially true for natural convection boundary layer fluxes. When unstructured pieces are used in these zones, they can cause significant skewness in corners and at geometry changes. Misha, (2020).

Due to the need for high dependability outcomes, it was important to create an efficient mesh with an appropriate number of nodes and elements, as indicated in the Figure 3 and Figure 4. However, a comparative analysis was performed between a variety of meshes with different qualities and numbers of elements, as shown in Table 2, to verify the efficiency of the mesh in this work. As a result, the mesh 1 model was chosen with the previously mentioned high-quality ratings.

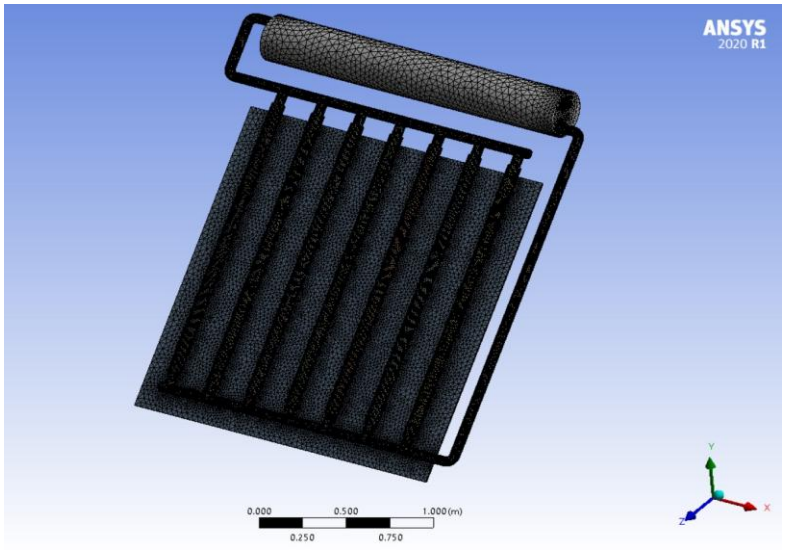

Figure 3. Meshing part of the conventional tube SWH

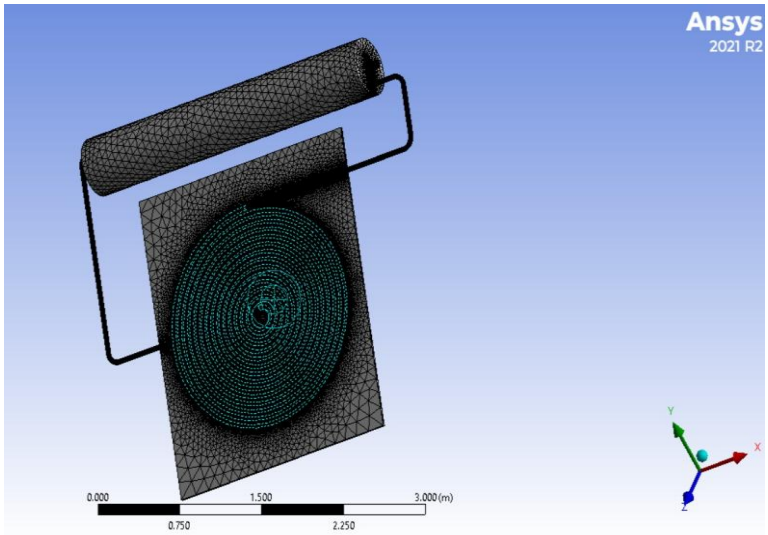

Figure 4. Meshing part of spiral tube SWH

Determination of design month

From the observations in the Table 2, August and September have the lowest value of irradiance yearly. Better performance during other months of the year would be made possible by using irradiance values from these two months in the system design. As a result, the month of August is chosen as the design month.

Table 2. Monthly Solar irradiance of Sokoto

Month	Global Horizontal Irradiance (GHI) (kWh/m^2 /day)
January	5.7
February	6.3
March	6.6
April	6.5
May	6.1
June	5.7
July	5.4
August	5.1
September	5.2
October	5.7
November	5.7
December	5.5

The monthly average daily solar radiations on the collector surface divided by the monthly average daily solar system load are known as the energy ratio E_R, and it is given by the equation 1

$$E_R = \frac{H_T}{Q_S} \qquad 1$$

Where H_T is the monthly average solar radiation on the collector surface (KJ/m^2 day) Q_S is the monthly average daily load (KJ/day)

The computation of system design parameters and subsequent component sizing was done based on the design month average daily solar radiation and meteorological data of Sokoto since the demand on the system during the design month is typically the highest by using equation 1. To establish the design month, the weather data processor's monthly average daily weather data and solar radiations on the collector's surface for all months were used. To determine the energy ratio, E_R programming codes were generated using the ANSYS software as input.

System Performance Simulation

Typical Meteorological Year (TMY) weather data for the location (Sokoto) and the system attributes listed in Table 3. were used to numerically simulate the system's performance.

Performance Analysis

Performance analysis is critical for determining if a system is fulfilling its function well and whether it is profitable. It enables specialists to understand which technology performs better, which heat transfer fluid is more efficient, and what the system's limitations are.

The temperatures inlet and outlet with mass flow rate was measured and Equation 2 was used to compute the performance

$$Q_u = mc_p(T_{f_0} - T_{f_i}) \qquad \mathbf{2}$$

Where, $Q_u$is the rate of useful energy gained, m is the mass flow rate of fluid flow, $C_p$is the heat capacity of water or working fluid and $T_{f_0}$and T_{f_i} are the inlet and outlet fluid temperature of the solar collector. The useful energy can also be expressed in terms of the energy absorbed by the absorber and the energy lost from the absorber as given by

$$Q_u = A_C F_R[I(\tau\alpha) - U_L(Tf_i - T_a)] \qquad \mathbf{3}$$

Where F_R is the 'collector heat removal factor' defined as the ratio of the actual heat transfer to the maximum possible rate, A_C is the surface area of the solar collector, I is the global solar radiation, is the absorptance–transmittance product, U_L is the overall loss coefficient of solar collector, and T_a is the ambient temperature.

$$Q_u = A_C F_R[I(\tau\alpha) - U_L(Tf_i - T_a)] \quad \textbf{4}$$

The relation between the collector efficiency factor and the heat removal factor F_R will be determine using Equation 5

$$F_R = \frac{mc_p}{A_C U_L}\left[1 - exp\left(-A_C U_L F/mC_p\right)\right] \quad \textbf{5}$$

The instantaneous collector efficiency relates the useful energy to the total radiation incident on the collector surface by Equation 6

$$\eta = \frac{T_{out} - T_{in}}{T_{out}} \text{ x } 100 \quad \textbf{6}$$

T_{out} Is the temperature of the hot water exiting the solar collector? T_{in} is the temperature of the cold water entering the collector.

$$\eta = \frac{\dot{m}c_p\Delta T}{IA_c} \quad \textbf{7}$$

where I is solar irradiation, η represents collector efficiency, ṁ is the mass flow rate, and A_c represents collector area, T is the temperature change, and it is measured in square metres m^2.

Efficiency is typically less than 100% because there are inefficiencies such as friction and heat loss, which convert the energy into alternative forms. Equation 7 was used to determine the efficiencies of the systems. When the efficiency test is performed, the range of tested temperatures, a straight line will result from a solar collector where the temperature of the fluid entering the collector equals the ambient temperature, i.e., the resultant of the collector efficiency is at its maximum.

Data Processing and Analysis

Temperatures at the inlet and outlet, solar radiation, collector size, and storage tank capacity were measured and observed using standard measuring tools that have been validated and are pertinent to the variables under investigation. The Origin software was utilized to process the gathered data. The data presented herein includes tables and graphs, such as line and bar graphs. The impact of storage tank capacity, collector size, collector orientation, and inlet and outlet temperatures was examined, and conclusions regarding the operation of solar water heaters were drawn based on the research findings. The data in this study were analyzed using ANSYS software, which was then used to calculate the analysis of a solar water heating system and calculate the savings obtained through the use of SWH. A dynamic software tool called ANSYS is used to simulate and optimize solar thermal systems, including those for space heating and hot water. Two different tube arrangements—spiral, straight- are the foundation for the ANSYS approach used in this research to simulate and analyze the performance of the solar water heating system.

Results and Discussions

This section presents the results of the simulation analysis and findings of the designed solar water heating system.

The ambient Temperatures fitted with solar water heater were recorded at one-hour intervals between 7.00 hours and 17:00 hours in this study.

The analytical findings include a calculation of the energy produced by the solar water heater and needed for the systems. The results of the simulation are shown in the Figures below, which also show the direction of water flow between outlet and inlet at different mass flow rates as well as values for temperature contour, pressure contour, velocity stream, velocity contour, and volume rendering profile of the collectors. After providing the software with all the necessary data, such as the properties of the different tube arrangements shown in the tables and figures, it carried out the calculations and outputted the results in the form of graphs, reports, and contours for the parameter distribution. The quantity of energy received in locations differs due to factors such as latitude, altitude, atmospheric conditions, and more. To gather data on radiation levels, it is necessary to determine the latitude and longitude of a place. This enables us to calculate the amount of sunlight received from the sun on a yearly basis at different angles and slopes, for the desired location. In this study, Sokoto, Sokoto State, Nigeria, is a case study.

Figure 5 shows the average monthly irradiation of Sokoto, Sokoto State, Nigeria, with latitude 13º03 N and longitude 5º14 E. The total daily incident of solar radiation that strikes the ground over a large region is covered in this section, taking into consideration seasonal changes in day length, the Sun's position above the horizon, and absorption by clouds and other atmospheric components. Ultraviolet and visible light both fall within the category of shortwave radiation. Over the year, there is some seasonal fluctuation in the average daily incident shortwave solar energy.

The brighter period of the year lasts from February 21st to April 26th, with an average daily incident shortwave energy per square meter above 6.4 kWh. The brightest month of the year in Sokoto is March, with an average of 6.6 kWh.

Figure 4, however, shows that the darker period of the year lasts from July 15 to September 29, with an average daily incident shortwave energy per square meter below 5.4 kWh. The darkest month of the year in Sokoto is August, with an average of 5.1 kWh.

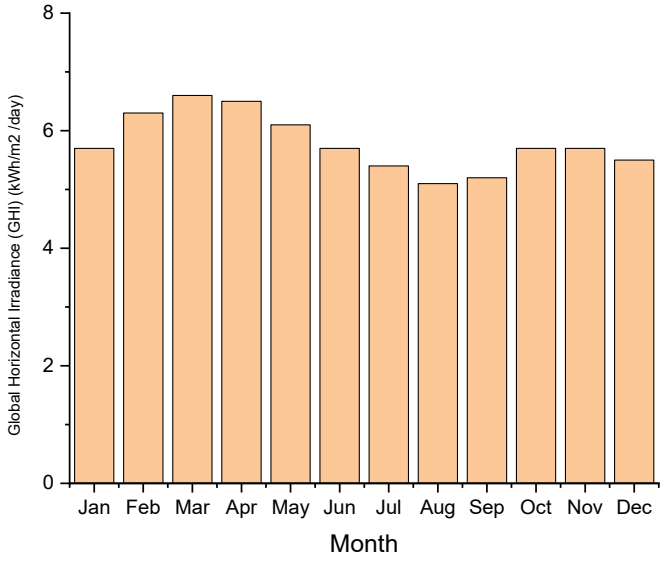

Figure 5: Average monthly solar Irradiation

The temperature contour, pressure contour, and airflow velocity at all node sites in the model duct were all measured using ANSYS FLUENT 2021 R2.

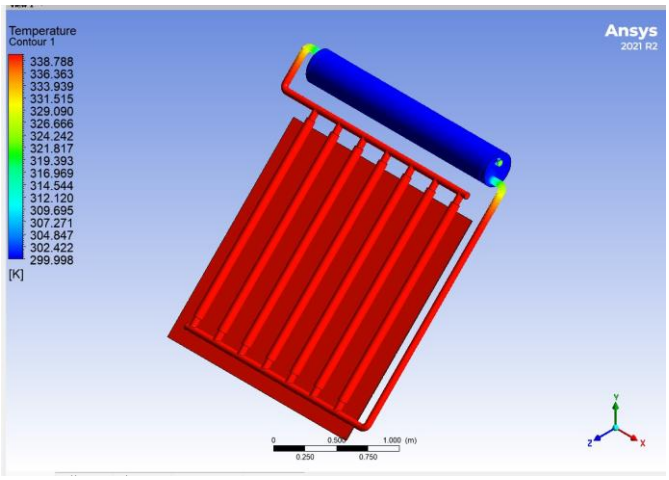

Figure 6: Temperature profile obtained from the conventional SWH

Figure 6 describes the temperature contour of a conventional solar water heater. The Figure also illustrates how the output contour temperature of the fluid domain portions was displayed in colour, with a temperature of 338.7K. The displayed value varied based on changes in the locations of the places where the temperature contour varied. In the legend, blue color represents the lowest temperature while the red color indicates the maximum temperature.

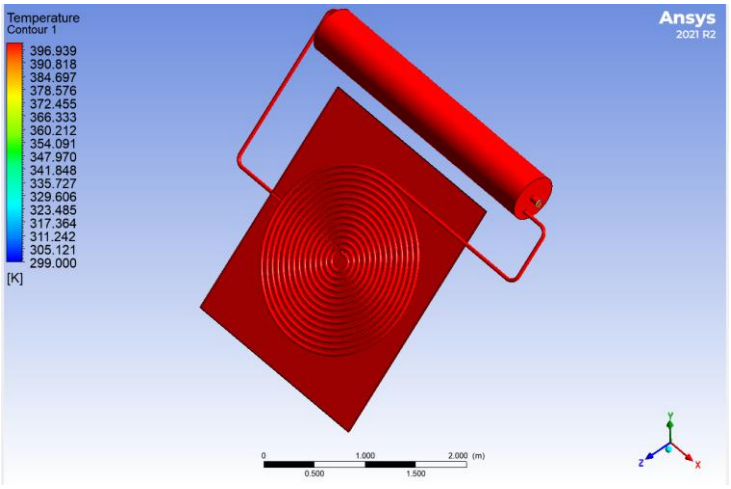

Figure 7: Temperature profile obtained from the spiral tube SWH

Figure 7 demonstrates the temperature contour of the solar water heater with a spiral tube arrangement, with the inlet coming from the far-left end of the model and the heat source coming from the top. The Figure, however, shows the temperature contour of a solar water heater, with the heat source coming from above and the inlet coming from the far end of the model. In the legend on the left side of the model, blue represents the least value and red represents the maximum value. The highest temperature, 338.788 K, for a straight tube, 396.939k K for spiral, and 400 K for zigzag arrangements. On this note, the zigzag tube records the highest temperature.

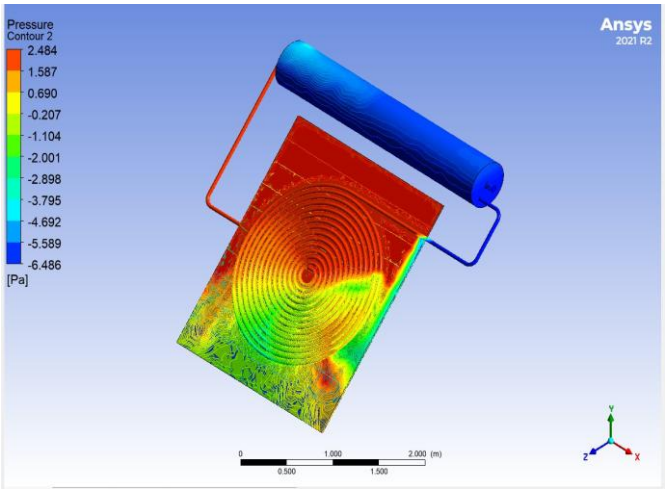

Figure 8: Pressure contour of spiral tube

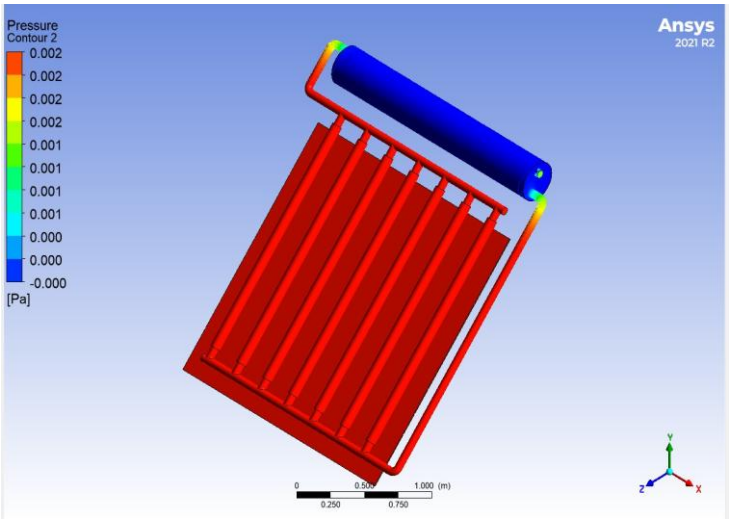

Figure 9: Pressure Contour of conventional SWH

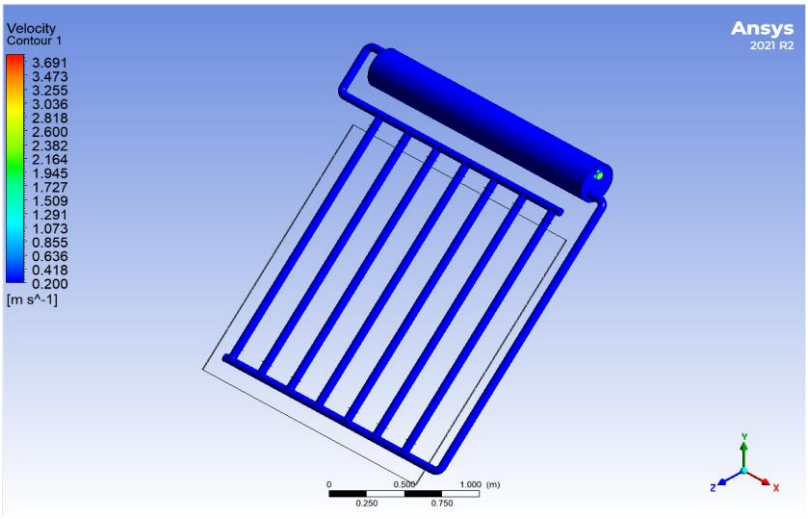

Figure 10: Velocity Contour of Conventional Tube SWH

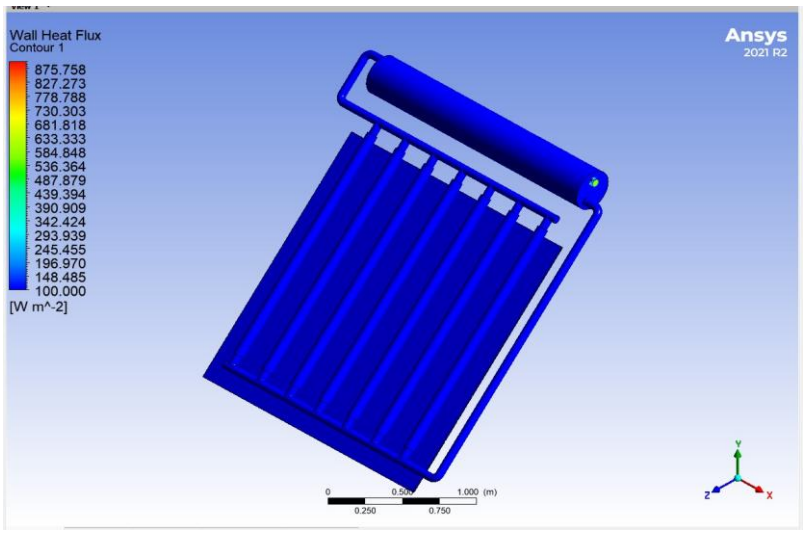

Figure 11: Heat Flux Contour For conventional SWH

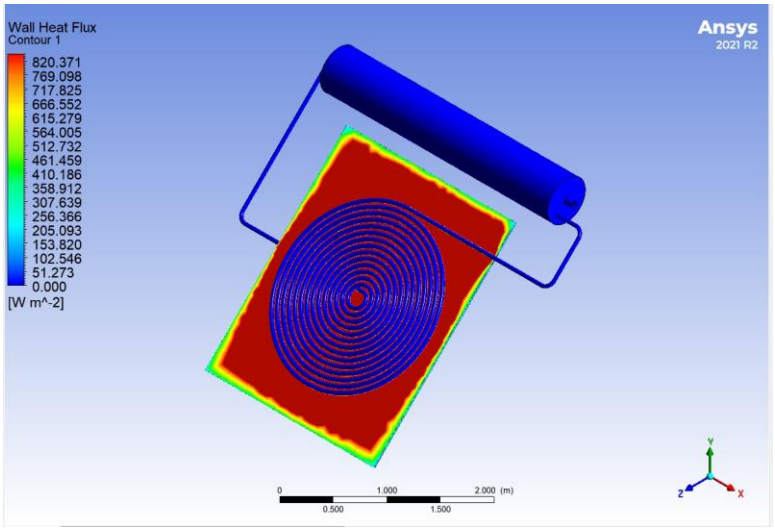

Figure 12: Heat Flux Contour for Spiral Tube SWH

The ambient temperatures of the solar water heater were tracked for this study at one-hour intervals between the hours of 7:00 hours and 17: 00 hours.

From the Figure 15, it is seen that outlet temperature rises slowly during the first few hours, but then increases until its peak at 12:00 hours. It is worth noting that the irradiance levels peak an hour before the outlet temperature. The highest outlet temperature attained is solar water heater with straight tube arrangement with 68ºC at about 12:00 hours, while solar water heater with spiral tube arrangement recorded 60ºC at the same time. It can be noted that there is a close relationship between a solar water heater with a straight tube arrangement and a solar water heater with a Spiral arrangement. From the graph, it is evident that the tube arrangements have a significant impact on the temperature of solar water heaters.

Figure 15, however, shows that temperature rise varies according to the time of day. As time passes, the isolation increases, as does the temperature, with the highest values observed at 13:00 hours in all tube arrangements, and then the temperature begins to decline from 15.00 hours to 16.00 hours.

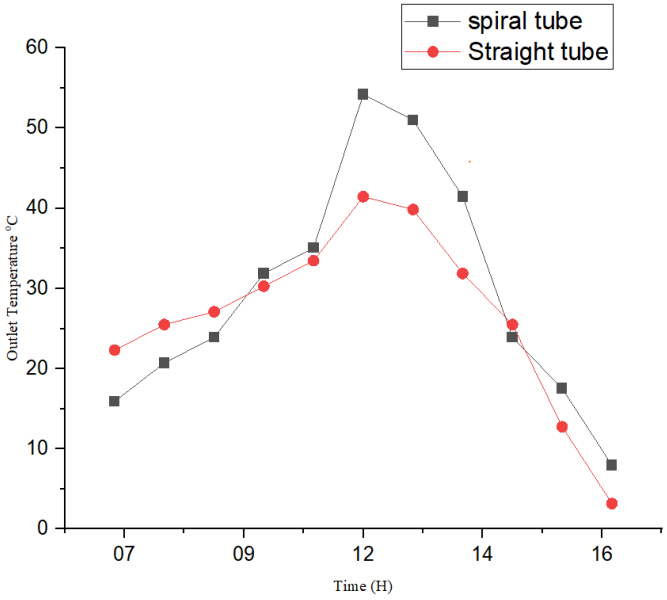

Figure 13: Graph of Efficiencies against Time

Figure 13, illustrates that the solar water heater with Spiral tube arrangement has the highest efficiency of about 54% at 12:00 hours and 41% at 12:00 this is also the peak time of the day. Equation 7 was used to calculate the efficiencies of the systems. The highest efficiency of a conventional solar water heater is 54%. Is safe to say that the solar water heater with a straight tube arrangement has the lowest efficiency at 41%.

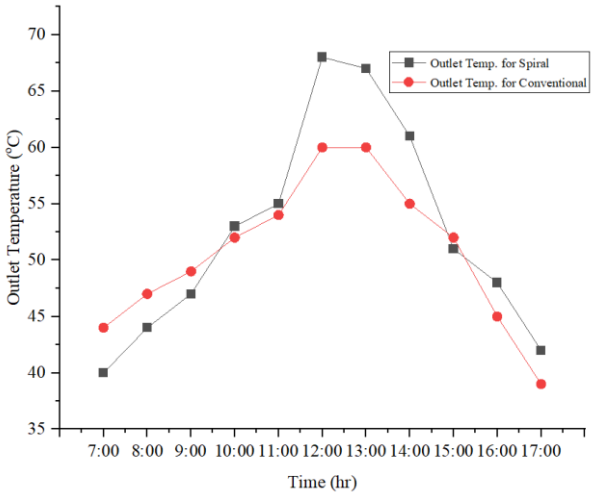

Figure 14: Graph of Outlet Temperatures against Time

Figure 14 demonstrates that the irradiance peaks between 12:00 and 13:00, then remains steady until 14:00 hours, after which it steadily decreases. At noon, the outlet temperature hits a high of 68ºC at about 12:00 hours with a solar water heater with straight tube arrangement and spiral tube arrangement recorded at 60ºC at the same time. The analytical results revealed that the solar irradiance levels and the outlet temperature are intimately unified.

Conclusion

In the current study, the performance of analysis of solar water heaters with different tube arrangements was analyzed using CFD simulation software (ANSYS FLUENT). Several simulations were run using solar radiation of Sokoto, Sokoto state, at various times, which has an impact on the working fluid's ability to transfer thermal energy and produce a range of results.

ANSYS Fluent was used to simulate the solar water heater in order to compare and forecast the system performance, guarantee system efficiency, and make all required adjustments to achieve the highest possible system performance.

From the result above, it is clear that conventional Solar water heater recorded the lowest outlet temperature, 60^0 C while solar water heater with Spiral tube arrangement recorded 68^0C at 12:00 hours

Based on the research's findings, it can be concluded that, a solar water heater with a Spiral tube arrangement has the higher efficiency of about 54% compared to 41% at 12:00 hours for the conventional solar water heater. It can be concluded that the tube arrangement is very vital in the performance of solar water heaters.

References

1. Bukola O Bolaji (2006). Flow design and collector performance of a natural circulation solar water heater. *Journal of Engineering and Applied Sciences*. 1(1): 7-13.
2. Balaji, K., Ganesh K.P., Sakthivadivel, D., Vigneswaran, V.S., and Iniyan, S. (2019) "Experimental investigation on flat plate solar collector using frictionally engaged thermal performance enhancer in the absorber tube," *Renewable Energy*, vol. 142, pp. 62–72.
3. Bracamonte, M. B. J., Parada, J., Dimas, J, and Baritto, M. (2015) "Effect of the collector tilt angle on thermal efficiency and stratification of passive water in glass evacuated tube solar water heater," *Applied Energy*, vol. 155, pp. 648–659.
4. Delfín, S. S., Carlos, R. E., and Valentín C. H. (2004) "Simulation of A Solar Domestic Water Heating System, With Different Collector Efficiencies and Different Volume Storage Tanks" *RE and PQJ.* Vol (1) (2) pp 124 – 130. https://doi.org/10.24084/repqj02.226
5. Eltaweel, M., Abdel-Rehim, A. A and Hussien, H. (2020) "Indirect thermosiphon flat-plate solar collector performance based on twisted tube design heat exchanger filled with nanofluid," *International Journal of Energy Research*, vol. 44, no. 6, pp. 4269–4278
6. Houri, A., (2006) "Solar water heating systems in Lebanon: current status and future prospects". *Renewable Energy: An Inter*. J., 31, 663-657
7. Ibrahim, A., Jin, G. L., Daghigh, R., Salleh, M. H. M., Othman, M.Y., Ruslan, H. (2009). "Hybrid photovoltaic thermal (PV/T) air and water-based solar collectors suitable for building integrated applications". *American Journal of Environmental Sciences,* 5 (2009), 618—624.

8. Ioannis, M. M. (1993) "Computer simulation and optimization of solar heating systems for Cyprus". Doctor of philosophy Thesis, School of Electronics and Manufacturing Systems Engineering, Faculty of Engineering and Science. University of Westminster.
9. Jaisankar, S., Ananth, J., Thulasi, S., Jayasuthakar, S.T. and Sheeba, K.N., (2011). "A comprehensive review on solar water heaters". *Renewable & Sustainable Energy Reviews*, 15, 3045-3050
10. Kangiwa, U. M., Mohammed, G., Hussaini, Z. and Umar, S. (2023). "Numerical Design of an Off-Grid Wind Energy Systems for Small Scale Residential Power Supply". *Journal of Energy Research and Reviews*, *15*(1), 47–57. https://doi.org/10.9734/jenrr/2023/v15i1297
11. Kishor, N., Das, M.K., Narain, A., and Ranjan, V.P. (2010) "Fuzzy model representation of thermosyphon solar water heating system", *Solar Energy*, 84 (6) 948-955.
12. Karthick, K. K. Murugavel, and P. Ramanan, (2018) "Performance enhancement of a building-integrated photovoltaic module using phase change material," *Energy*, vol. 142, pp. 803–812.
13. Kazuz M.R. (2014). "Hybrid solar thermos-electric systems for combined heat and power" PhD thesis .pdf. Cardiff University.
14. Manoj, P. K., K. Mylsamy, and P. T. (2020) "Saravanakumar, "Experimental investigations on thermal properties of nanoSiO2/paraffin phase change material (PCM) for solar thermal energy storage applications," *Energy Sources, Part A: Recovery, Utilization, and Environmental Effects*, vol. 42, no. 19, pp. 2420–2433.
15. Moravej, M., Saffarian, M. R., Li, K. B., Doranehgard, M. H., and Xiong, Q. (2020) "Experimental investigation of circular flat panel collector performance with spiral pipes," *Journal of Thermal Analysis and Calorimetry*, vol. 140, no. 3, pp. 1229– 1236.
16. Manoram, R. B., Moorthy, R. S., and Ragunathan, R. (2021) "Investigation on influence of dimpled surfaces on heat transfer enhancement and friction factor in solar water heater," *Journal of Thermal Analysis and Calorimetry*, vol. 145, no. 2, pp. 541–558.
17. Samson, A.A. (2013) Performance of Solar Water Heater in Akure, Nigeria. Journal of Energy Technologies and Policy, 3(6), 1-8.
18. Sakhaei, S. A., and Valipour, M. S. (2020) "Thermal performance analysis of a flat plate solar collector by utilizing helically corrugated risers: an experimental study," *Solar Energy*, vol. 207, pp. 235–246.
19. Sadeghi, O., Mohammed, H. A., Bakhtiari-Nejad, M and Wahid, M. A. (2016). "Heat transfer and nanofluid flow characteristics through a circular tube fitted with helical tape inserts," *International Communications in Heat and Mass Transfer*, vol. 71, pp. 234–244.
20. Silva, F. A. S., and Salviano, L. O (2019) "Heat transfer enhancement in a flat-plate solar water heater through longitudinal vortex generator," *Journal of Solar Energy Engineering*, vol. 141, no. 4.

CITATION

Hussaini, Z., Muhammad, M., Daniel, D., Audu, A. I., & Fakai, R. U. (2025). Performance Comparison of Solar Water Heaters with Zigzag and Spiral Tube Configurations Using ANSYS FLUENT. In Global Journal of Research in Agriculture & Life Sciences (Vol. 5, Number 5, pp. 22–34).

https://doi.org/10.5281/zenodo.17119079